

---

# COMPREHENSIVE EVALUATION OF NO-REFERENCE IMAGE QUALITY ASSESSMENT ALGORITHMS ON AUTHENTIC DISTORTIONS

---

Domonkos Varga

January 5, 2022

## ABSTRACT

Objective image quality assessment deals with the prediction of digital images' perceptual quality. No-reference image quality assessment predicts the quality of a given input image without any knowledge or information about its pristine (distortion free) counterpart. Machine learning algorithms are heavily used in no-reference image quality assessment because it is very complicated to model the human visual system's quality perception. Moreover, no-reference image quality assessment algorithms are evaluated on publicly available benchmark databases. These databases contain images with their corresponding quality scores. In this study, we evaluate several machine learning based NR-IQA methods and one opinion unaware method on databases consisting of authentic distortions. Specifically, LIVE In the Wild and KonIQ-10k databases were applied to evaluate the state-of-the-art. For machine learning based methods, appx. 80% were used for training and the remaining 20% were used for testing. Furthermore, average PLCC, SROCC, and KROCC values were reported over 100 random train-test splits. The statistics of PLCC, SROCC, and KROCC values were also published using boxplots. Our evaluation results may be helpful to obtain a clear understanding about the status of state-of-the-art no-reference image quality assessment methods.

**Keywords** no-reference image quality assessment

## 1 Introduction

After digital images are captured, they suffer from a wide variety of distortions due to compression, editing, retargeting, and transmission. The above mentioned mechanisms influence the perceived quality of digital images. *Objective image quality assessment (IQA)* deals with the measurement of perceptual image quality where image processing, computer vision, artificial intelligence, and machine learning techniques are applied to construct computational models to predict perceived image quality. Due to our limited understanding of the human visual system, it is very complicated to model the human visual system's quality perception. Thus, machine learning methods are heavily used to imitate the processes of such complex mechanisms of the human visual system. Since humans are the end users of digital images, the most reliable method to evaluate the quality of digital images is to ask humans for quality ratings of images. *Subjective IQA* deals with gathering subjective scores from human observers considering the recommendations of different international standards, such as ITU-R BT.500-11 [1] or ITU-P.910 [2]. Subsequently, the scores are processed to determine the mean opinion score (MOS) or the difference mean opinion score (DMOS). There are several IQA databases publicly available which contain images labelled with MOS or DMOS. Table 1 allows a comparison of publicly available IQA databases. The majority of IQA data sets contains a small set of pristine (distortion free) images and distorted images are derived from the pristine image using different artificial distortion types and levels. On the other hand, some databases (LIVE In the Wild [3] and KonIQ-10k [4]) consist of individual images with authentic distortions collected from the Internet or private collections. Objective IQA algorithms are trained and tested on these databases.

In this study, our goal is to evaluate several state-of-the-art no-reference image quality assessment (NR-IQA) algorithms, including BLIINDS-II [5], BMPRI [6], BRISQUE [7], CurveletQA [8], DIIVINE [9], ENIQA [10], GRAD-LOG-CP [11], GWH-GLBP-BIQA [12], IQVG [13], MultiGAP-GPR [14], MultiGAP-SVR [14], NBIQA [15], OG-IQA [16],

ORACLE [17], PIQE [18], SCORER [19], SEER [20], SPF-IQA [21], and SSEQ [22], on databases with authentic distortions. Excluding PIQE [18] which is an opinion-unaware method, all algorithms are machine learning based. Machine learning based algorithms were trained on appx. 80% of images and tested on the remaining 20%. Correlation between the predicted and the ground-truth scores was measured by Pearson’s linear correlation coefficient (PLCC), Spearman’s rank order correlation coefficient (SROCC), and Kendall’s rank order correlation coefficient (KROCC). In this study, we report on the average PLCC, SROCC, and KROCC values measured over 100 random train-test splits. Moreover, the statistics of PLCC, SROCC, and KROCC values are summarized with boxplots.

Table 1: Comparison of several publicly available IQA databases.

| Database                     | Ref. images | Test images | Resolution        | Distortion levels | Number of distortions |
|------------------------------|-------------|-------------|-------------------|-------------------|-----------------------|
| LIVE [23]                    | 29          | 779         | $768 \times 512$  | 4-5               | 5                     |
| A57 [24]                     | 3           | 54          | $512 \times 512$  | 6                 | 3                     |
| Toyoma-MICT [25]             | 14          | 168         | $768 \times 512$  | 6                 | 2                     |
| TID2008 [26]                 | 25          | 1,700       | $512 \times 384$  | 4                 | 17                    |
| CSIQ [27]                    | 30          | 866         | $512 \times 512$  | 4-5               | 6                     |
| VCL-FER [28]                 | 23          | 552         | $683 \times 512$  | 6                 | 4                     |
| LIVE Multiple Distorted [29] | 15          |             | $1280 \times 720$ | 3                 |                       |
| TID2013 [30]                 | 25          | 3,000       | $512 \times 384$  | 5                 | 24                    |
| CID:IQ [31]                  | 23          | 690         | $800 \times 800$  | 5                 | 6                     |
| LIVE In the Wild [3]         | -           | 1,169       | $500 \times 500$  | -                 | N/A                   |
| MDID [32]                    | 20          | 1,600       | $512 \times 384$  | 4                 | 5                     |
| KonIQ-10k [4]                | -           | 10,073      | $1024 \times 768$ | -                 | N/A                   |
| KADID-10k [33]               | 81          | 10,125      | $512 \times 384$  | 5                 | 25                    |

## 1.1 Contributions

The main contribution of this study is the comprehensive evaluation of several state-of-the-art NR-IQA algorithms (BLINDS-II [5], BMPRI [6], BRISQUE [7], CurveletQA [8], DIIVINE [9], ENIQA [10], GRAD-LOG-CP [11], GWH-GLBP-BIQA [12], IQVG [13], MultiGAP-GPR [14], MultiGAP-SVR [14], NBIQA [15], OG-IQA [16], ORACLE [17], PIQE [18], SCORER [19], SEER [20], SPF-IQA [21], and SSEQ [22]) on LIVE In the Wild and KonIQ-10k databases. Average PLCC, SROCC, and KROCC are reported measured over 100 random train-test splits (appx. 80% for training and 20% for testing). Moreover, the statistics of PLCC, SROCC, and KROCC values are summarized in box plots.

## 2 Experimental results

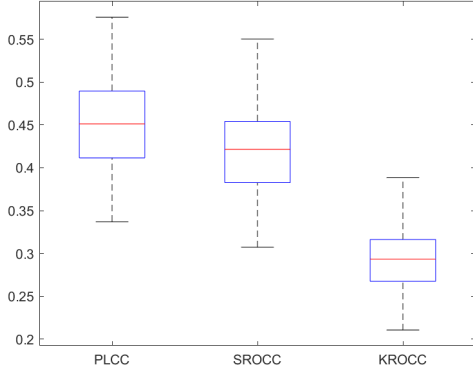
In this section, NR-IQA algorithms are evaluated on LIVE In the Wild and KonIQ-10k databases. As already mentioned, 80% of images was used for training and the remaining 20% for testing. Furthermore, average PLCC, SROCC, and KROCC values are reported measured over 100 random train-test splits.

### 2.1 LIVE In the Wild

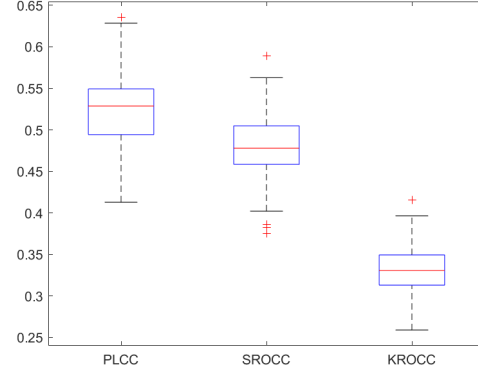
In this subsection, we present our results measured on LIVE In the Wild database. Average PLCC, SROCC, and KROCC are summarized in Table 2. It can be seen that MultiGAP [14] methods, which extracts deep features from Inception modules of an Inception-v3 convolutional neural network, achieve the best results. MultiGAP-SVR [14] utilizes an support vector regressor (SVR) with Gaussian kernel function, while MultiGAP-GPR [14], [34] relies on Gaussian process regression with rational quadratic kernel function. The statistics of PLCC, SROCC, and KROCC values are summarized in Figures 1, 2, and 3. On each box, the central mark indicates the median, and the bottom and top edges of the box indicate the 25th and 75th percentiles, respectively. The whiskers extend to the most extreme data points not considered outliers, and the outliers are plotted individually using the ‘+’ symbol.

### 2.2 KonIQ-10k

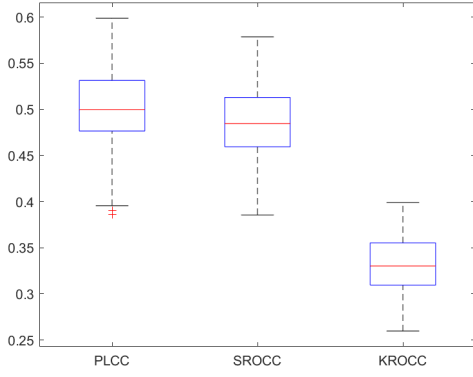
In this subsection, we present our results measured on KonIQ-10k database. Average PLCC, SROCC, and KROCC are summarized in Table 3. Similar to LIVE In the Wild, MultiGAP [14], [34] methods achieve the best performance. The statistics of PLCC, SROCC, and KROCC values are summarized in Figures 4, 5, and 6. As already mentioned, on



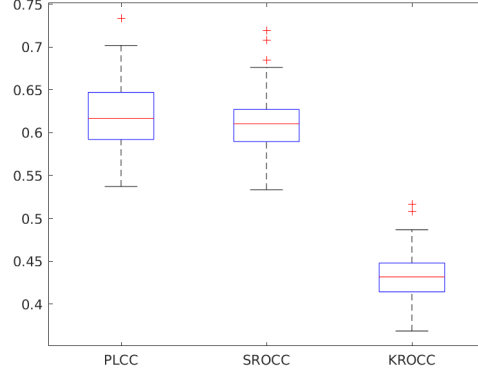
(a) BLIINDS-II.



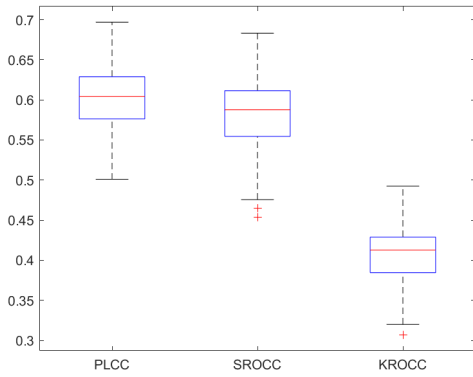
(b) BMPRI.



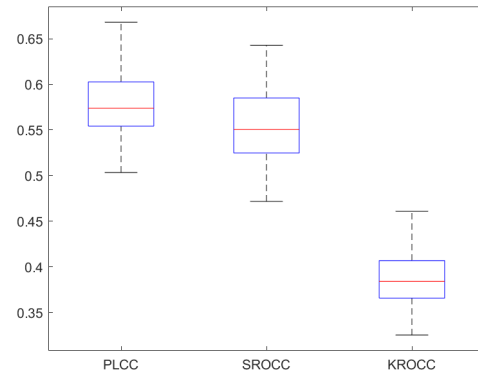
(c) BRISQUE.



(d) CurveletQA.

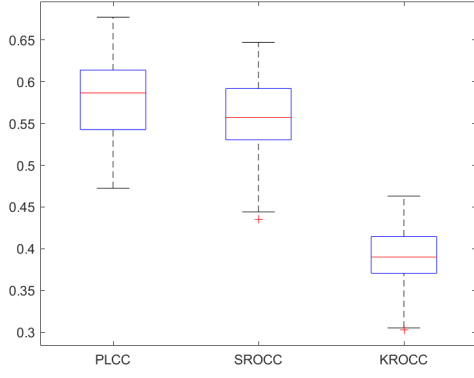


(e) DIIVINE.

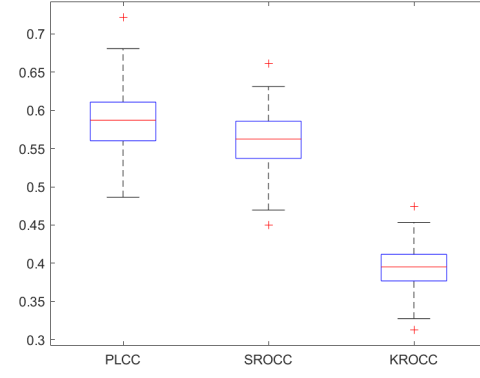


(f) ENIQA.

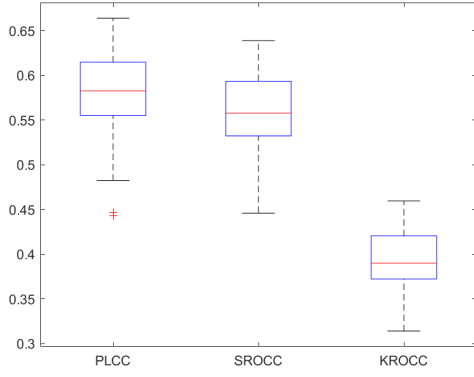
Figure 1: Box plots of the measured PLCC, SROCC, and KROCC values on LIVE In the Wild database. 100 random train-test splits.



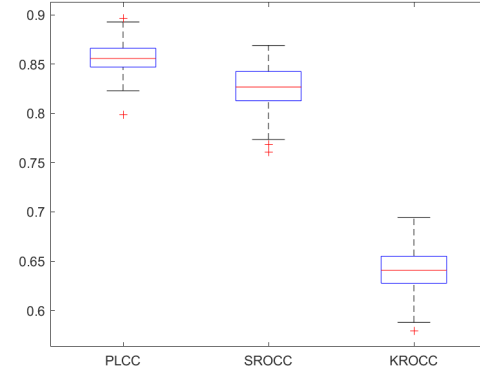
(a) GRAD-LOG-CP.



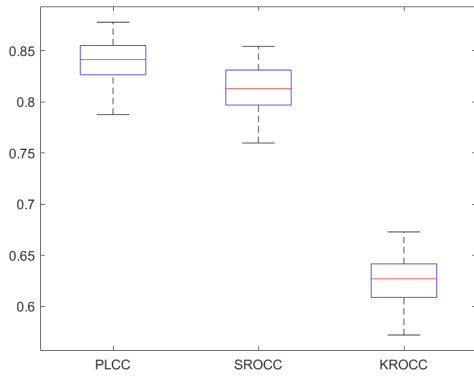
(b) GWH-GLBP-BIQA.



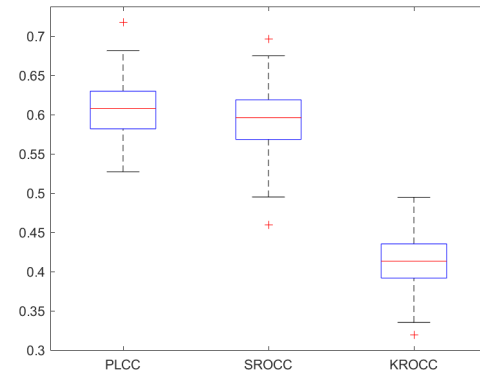
(c) IQVG.



(d) MultiGAP-GPR.

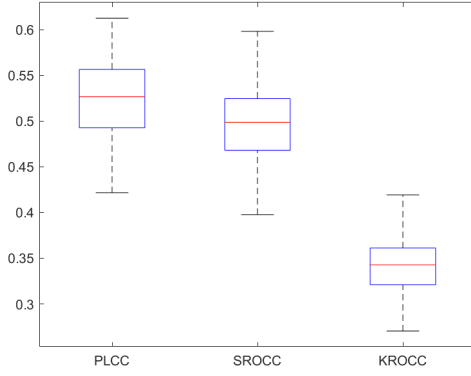


(e) MultiGAP-SVR.

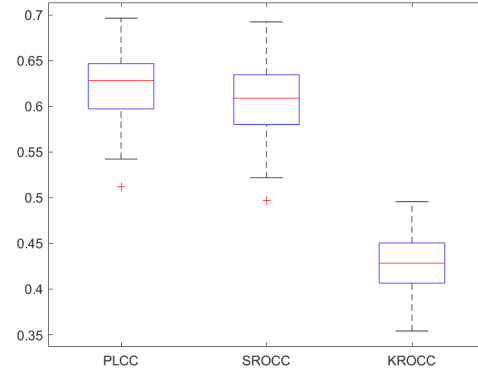


(f) NBIQA.

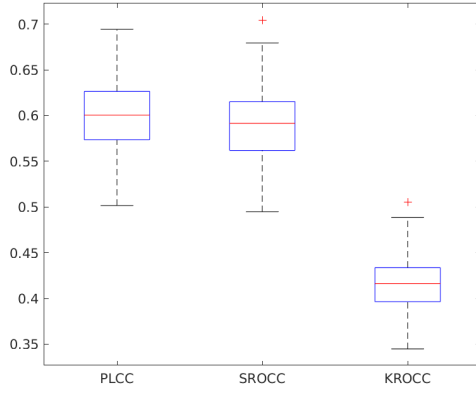
Figure 2: Box plots of the measured PLCC, SROCC, and KROCC values on LIVE In the Wild database. 100 random train-test splits.



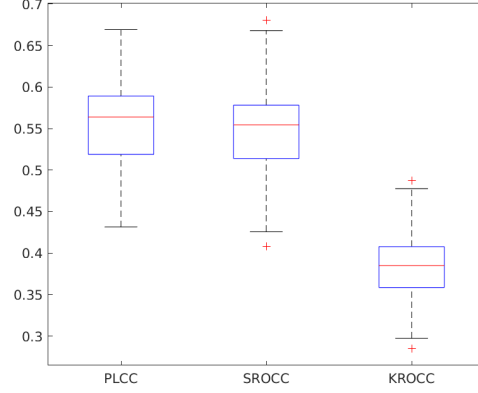
(a) OG-IQA.



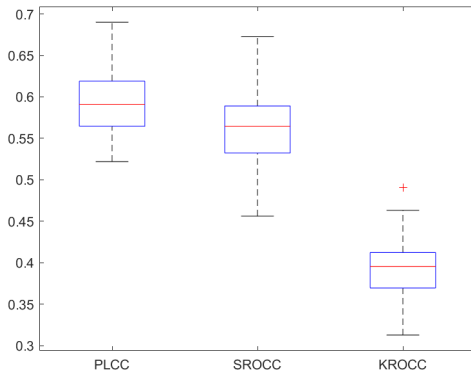
(b) ORACLE.



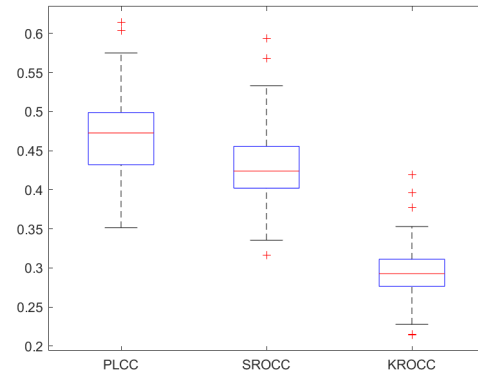
(c) SCORER.



(d) SEER.



(e) SPF-IQA.



(f) SSEQ.

Figure 3: Box plots of the measured PLCC, SROCC, and KROCC values on LIVE In the Wild database. 100 random train-test splits.

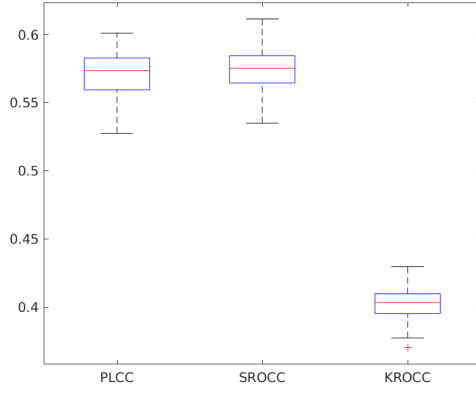
Table 2: Overall performance on LIVE In the Wild. Average PLCC, SROCC, and KROCC are reported, measured 100 random train-test splits. The best results are typed by **bold**, the second best results are typed by *italic*, the third best results are underlined.

| Method                  | PLCC         | SROCC        | KROCC        |
|-------------------------|--------------|--------------|--------------|
| BLIINDS-II [5]          | 0.450        | 0.419        | 0.292        |
| BMPRI [6]               | 0.521        | 0.480        | 0.332        |
| BRISQUE [7]             | 0.503        | 0.487        | 0.333        |
| CurveletQA [8]          | 0.620        | <u>0.611</u> | <u>0.433</u> |
| DIIVINE [9]             | 0.602        | <u>0.579</u> | 0.405        |
| ENIQA [10]              | 0.578        | 0.554        | 0.386        |
| GRAD-LOG-CP [11]        | 0.579        | 0.557        | 0.391        |
| GWH-GLBP-BIQA [12]      | 0.588        | 0.560        | 0.394        |
| IQVG [13]               | 0.581        | 0.559        | 0.393        |
| MultiGAP-SVR [14]       | <i>0.841</i> | <i>0.813</i> | <i>0.626</i> |
| MultiGAP-GPR [14], [34] | <b>0.857</b> | <b>0.826</b> | <b>0.641</b> |
| NBIQA [15]              | 0.607        | 0.593        | 0.414        |
| OG-IQA [16]             | 0.526        | 0.497        | 0.342        |
| ORACLE [17]             | <u>0.622</u> | 0.606        | 0.427        |
| PIQE [18]               | 0.171        | 0.108        | 0.070        |
| SCORER [19]             | 0.599        | 0.590        | 0.416        |
| SEER [20]               | 0.556        | 0.547        | 0.383        |
| SPF-IQA [21]            | 0.592        | 0.563        | 0.395        |
| SSEQ [22]               | 0.469        | 0.429        | 0.295        |

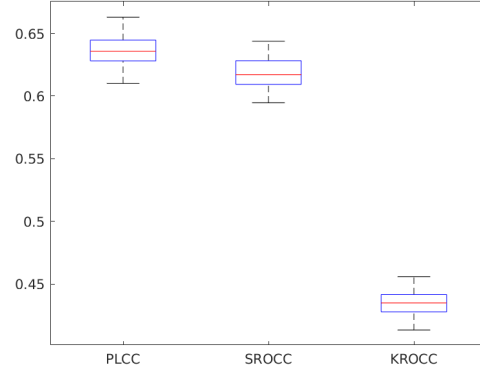
each box, the central mark indicates the median, and the bottom and top edges of the box indicate the 25<sup>th</sup> and 75<sup>th</sup> percentiles, respectively. The whiskers extend to the most extreme data points not considered outliers, and the outliers are plotted individually using the '+' symbol.

Table 3: Overall performance on KonIQ-10k. Average PLCC, SROCC, and KROCC are reported, measured 100 random train-test splits. The best results are typed by **bold**, the second best results are typed by *italic*, the third best results are underlined.

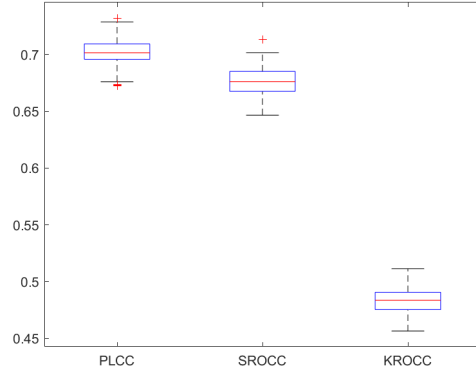
| Method                  | PLCC         | SROCC        | KROCC        |
|-------------------------|--------------|--------------|--------------|
| BLIINDS-II [5]          | 0.571        | 0.575        | 0.403        |
| BMPRI [6]               | 0.636        | 0.619        | 0.435        |
| BRISQUE [7]             | 0.702        | 0.676        | 0.483        |
| CurveletQA [8]          | 0.728        | 0.716        | 0.520        |
| DIIVINE [9]             | 0.709        | 0.692        | 0.498        |
| ENIQA [10]              | 0.758        | 0.744        | 0.546        |
| GRAD-LOG-CP [11]        | 0.705        | 0.698        | 0.502        |
| GWH-GLBP-BIQA [12]      | 0.726        | 0.700        | 0.508        |
| IQVG [13]               | 0.688        | 0.684        | 0.489        |
| MultiGAP-SVR [14]       | <i>0.915</i> | <i>0.911</i> | <i>0.732</i> |
| MultiGAP-GPR [14], [34] | <b>0.928</b> | <b>0.925</b> | <b>0.752</b> |
| NBIQA [15]              | 0.770        | 0.748        | 0.549        |
| OG-IQA [16]             | 0.652        | 0.635        | 0.448        |
| ORACLE [17]             | 0.757        | 0.748        | 0.550        |
| PIQE [18]               | 0.206        | 0.245        | 0.165        |
| SCORER [19]             | <u>0.772</u> | <u>0.762</u> | <u>0.561</u> |
| SEER [20]               | 0.705        | 0.705        | 0.509        |
| SPF-IQA [21]            | 0.759        | 0.740        | 0.543        |
| SSEQ [22]               | 0.584        | 0.573        | 0.402        |



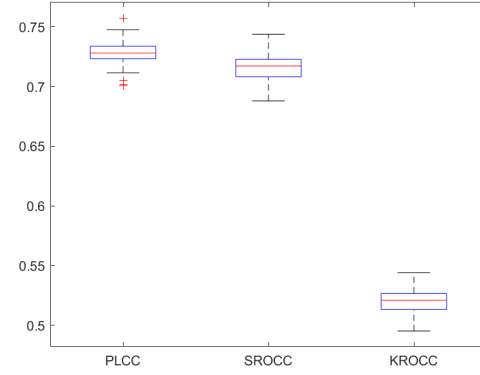
(a) BLIINDS-II.



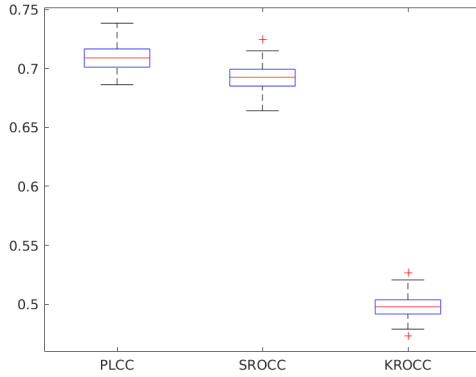
(b) BMPRI.



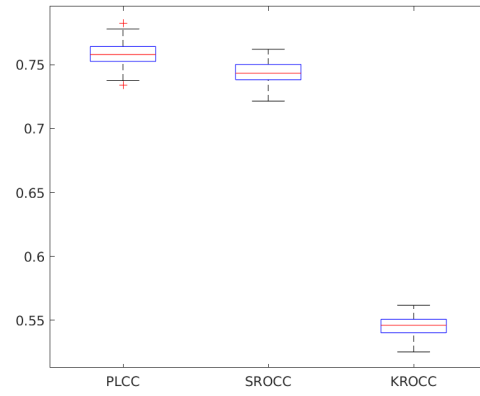
(c) BRISQUE.



(d) CurveletQA.

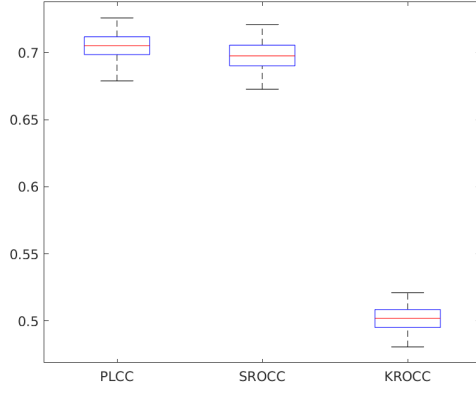


(e) DIIVINE.

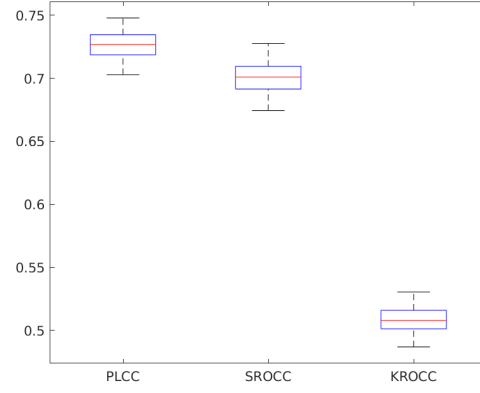


(f) ENIQA.

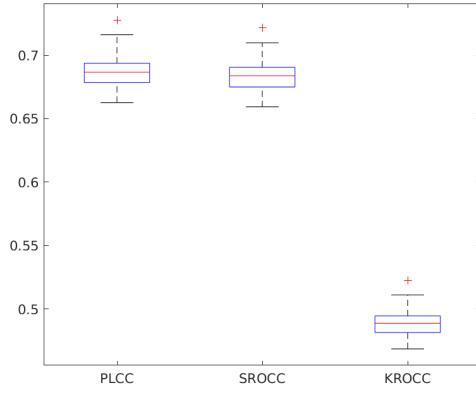
Figure 4: Box plots of the measured PLCC, SROCC, and KROCC values on KonIQ-10k database. 100 random train-test splits.



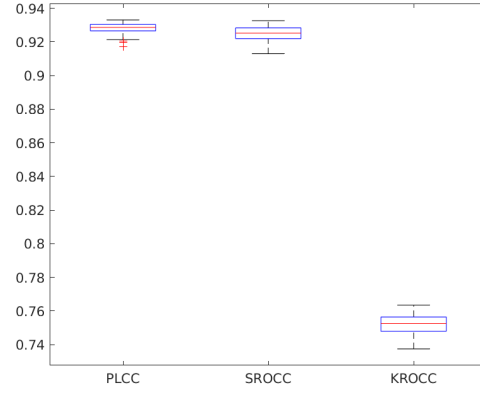
(a) GRAD-LOG-CP.



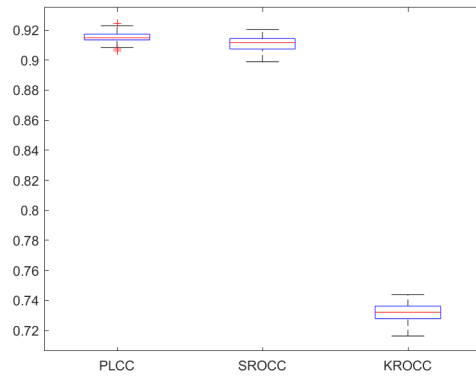
(b) GWH-GLBP-BIQA.



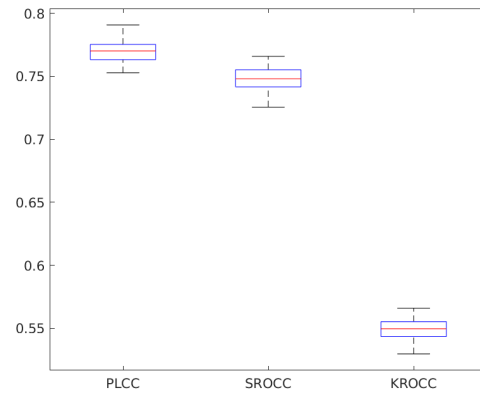
(c) IQVG.



(d) MultiGAP-GPR.



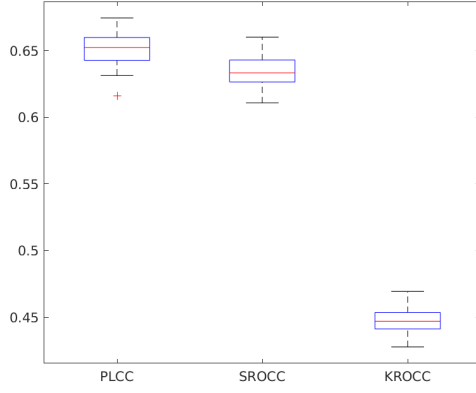
(e) MultiGAP-SVR.



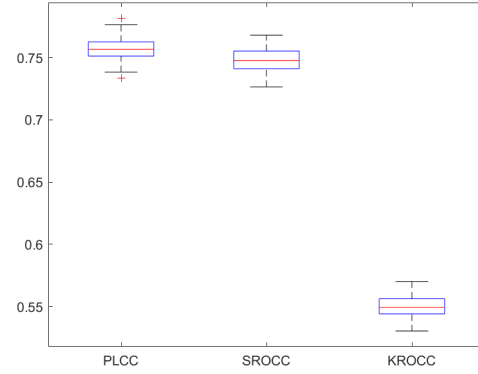
(f) NBIQA.

Figure 5: Box plots of the measured PLCC, SROCC, and KROCC values on KonIQ-10k database. 100 random train-test splits.

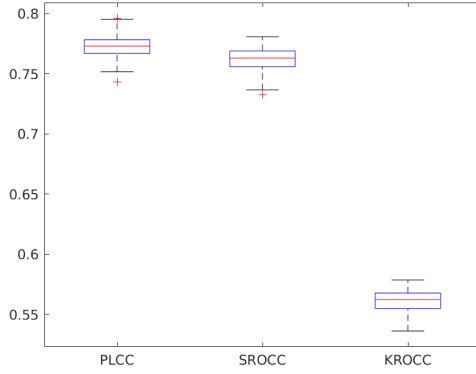




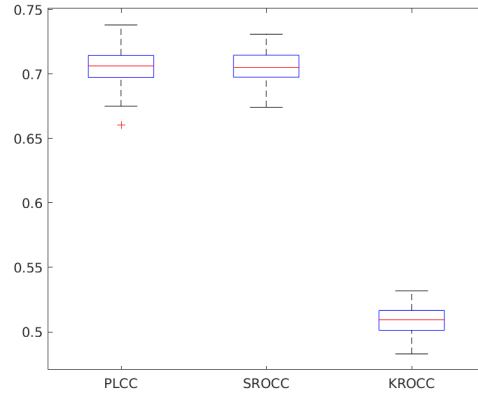
(a) OG-IQA.



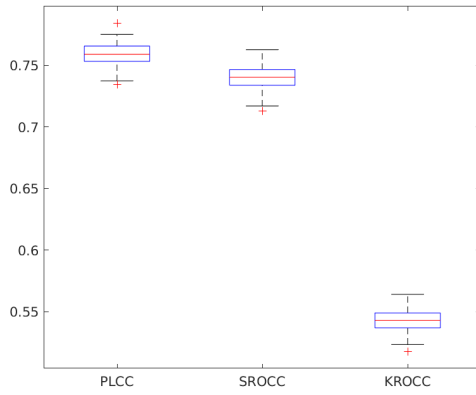
(b) ORACLE.



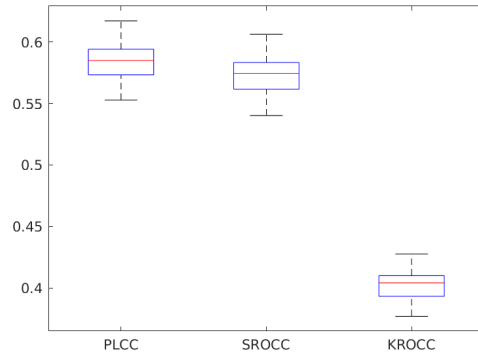
(c) SCORER.



(d) SEER.



(e) SPF-IQA.



(f) SSEQ.

Figure 6: Box plots of the measured PLCC, SROCC, and KROCC values on KonIQ-10k database. 100 random train-test splits.

### 3 Conclusion

In this study, we evaluated several NR-IQA algorithms on authentic distortions. Specifically, we utilized two publicly available benchmark databases (LIVE In the Wild and KonIQ-10k) to evaluate the state-of-the-art in NR-IQA. Appx. 80% of images were used for training and the remaining 20% were used for testing. Average PLCC, SROCC, and KROCC values were reported measured over 100 random train-test splits. Moreover, the boxplots of PLCC, SROCC, and KROCC values were also published for each examined machine learning based method. Our evaluation results may be helpful to obtain a clear understanding about the status of state-of-the-art no-reference image quality assessment methods.

### References

- [1] RECOMMENDATION ITU-R BT. Methodology for the subjective assessment of the quality of television pictures. 2002.
- [2] P ITU-T RECOMMENDATION. Subjective video quality assessment methods for multimedia applications. *International telecommunication union*, 1999.
- [3] Deepti Ghadiyaram and Alan C Bovik. Massive online crowdsourced study of subjective and objective picture quality. *IEEE Transactions on Image Processing*, 25(1):372–387, 2015.
- [4] Hanhe Lin, Vlad Hosu, and Dietmar Saupe. Koniq-10k: Towards an ecologically valid and large-scale iqa database. *arXiv preprint arXiv:1803.08489*, 2018.
- [5] Michele A Saad, Alan C Bovik, and Christophe Charrier. Blind image quality assessment: A natural scene statistics approach in the dct domain. *IEEE transactions on Image Processing*, 21(8):3339–3352, 2012.
- [6] Xiongkuo Min, Guangtao Zhai, Ke Gu, Yutao Liu, and Xiaokang Yang. Blind image quality estimation via distortion aggravation. *IEEE Transactions on Broadcasting*, 64(2):508–517, 2018.
- [7] Anish Mittal, Anush Krishna Moorthy, and Alan Conrad Bovik. No-reference image quality assessment in the spatial domain. *IEEE Transactions on image processing*, 21(12):4695–4708, 2012.
- [8] Lixiong Liu, Hongping Dong, Hua Huang, and Alan C Bovik. No-reference image quality assessment in curvelet domain. *Signal Processing: Image Communication*, 29(4):494–505, 2014.
- [9] Anush Krishna Moorthy and Alan Conrad Bovik. Blind image quality assessment: From natural scene statistics to perceptual quality. *IEEE transactions on Image Processing*, 20(12):3350–3364, 2011.
- [10] Xiaoqiao Chen, Qingyi Zhang, Manhui Lin, Guangyi Yang, and Chu He. No-reference color image quality assessment: from entropy to perceptual quality. *EURASIP Journal on Image and Video Processing*, 2019(1):77, 2019.
- [11] Wufeng Xue, Xuanqin Mou, Lei Zhang, Alan C Bovik, and Xiangchu Feng. Blind image quality assessment using joint statistics of gradient magnitude and laplacian features. *IEEE Transactions on Image Processing*, 23(11):4850–4862, 2014.
- [12] Qiaohong Li, Weisi Lin, and Yuming Fang. No-reference quality assessment for multiply-distorted images in gradient domain. *IEEE Signal Processing Letters*, 23(4):541–545, 2016.
- [13] Zhongyi Gu, Lin Zhang, and Hongyu Li. Learning a blind image quality index based on visual saliency guided sampling and gabor filtering. In *2013 IEEE International Conference on Image Processing*, pages 186–190. IEEE, 2013.
- [14] Domonkos Varga. Multi-pooled inception features for no-reference image quality assessment. *Applied Sciences*, 10(6):2186, 2020.
- [15] Fu-Zhao Ou, Yuan-Gen Wang, and Guopu Zhu. A novel blind image quality assessment method based on refined natural scene statistics. In *2019 IEEE International Conference on Image Processing (ICIP)*, pages 1004–1008. IEEE, 2019.
- [16] Lixiong Liu, Yi Hua, Qingjie Zhao, Hua Huang, and Alan Conrad Bovik. Blind image quality assessment by relative gradient statistics and adaboosting neural network. *Signal Processing: Image Communication*, 40:1–15, 2016.
- [17] Mariusz Oszust. Optimized filtering with binary descriptor for blind image quality assessment. *IEEE Access*, 6:42917–42929, 2018.

- [18] N Venkatanath, D Praneeth, Maruthi Chandrasekhar Bh, Sumohana S Channappayya, and Swarup S Medasani. Blind image quality evaluation using perception based features. In *2015 Twenty First National Conference on Communications (NCC)*, pages 1–6. IEEE, 2015.
- [19] Mariusz Oszust. Local feature descriptor and derivative filters for blind image quality assessment. *IEEE Signal Processing Letters*, 26(2):322–326, 2019.
- [20] Mariusz Oszust. No-reference image quality assessment with local gradient orientations. *Symmetry*, 11(1):95, 2019.
- [21] Domonkos Varga. No-reference image quality assessment based on the fusion of statistical and perceptual features. *Journal of Imaging*, 6(8):75, 2020.
- [22] Lixiong Liu, Bao Liu, Hua Huang, and Alan Conrad Bovik. No-reference image quality assessment based on spatial and spectral entropies. *Signal Processing: Image Communication*, 29(8):856–863, 2014.
- [23] Hamid R Sheikh, Muhammad F Sabir, and Alan C Bovik. A statistical evaluation of recent full reference image quality assessment algorithms. *IEEE Transactions on image processing*, 15(11):3440–3451, 2006.
- [24] Damon M Chandler and Sheila S Hemami. Vsnr: A wavelet-based visual signal-to-noise ratio for natural images. *IEEE transactions on image processing*, 16(9):2284–2298, 2007.
- [25] Yuukou Horita, Keiji Shibata, Yoshikazu Kawayoke, and ZM Parvez Sazzad. Mict image quality evaluation database. *Online*, <http://mict.eng.u-toyama.ac.jp/mictdb.html>, 2011.
- [26] Nikolay Ponomarenko, Vladimir Lukin, Alexander Zelensky, Karen Egiazarian, Marco Carli, and Federica Battisti. Tid2008-a database for evaluation of full-reference visual quality assessment metrics. *Advances of Modern Radioelectronics*, 10(4):30–45, 2009.
- [27] Eric Cooper Larson and Damon Michael Chandler. Most apparent distortion: full-reference image quality assessment and the role of strategy. *Journal of electronic imaging*, 19(1):011006, 2010.
- [28] Anđela Zarić, Nenad Tatalović, Nikolina Brajković, Hrvoje Hlevnjak, Matej Lončarić, Emil Dumić, and Sonja Grgić. Vcl@fer image quality assessment database. *AUTOMATIKA: časopis za automatiku, mjerenje, elektroniku, računarstvo i komunikacije*, 53(4):344–354, 2012.
- [29] Dinesh Jayaraman, Anish Mittal, Anush K Moorthy, and Alan C Bovik. Objective quality assessment of multiply distorted images. In *2012 Conference record of the forty sixth asilomar conference on signals, systems and computers (ASILOMAR)*, pages 1693–1697. IEEE, 2012.
- [30] Nikolay Ponomarenko, Lina Jin, Oleg Ieremeiev, Vladimir Lukin, Karen Egiazarian, Jaakko Astola, Benoit Vozel, Kacem Chehdi, Marco Carli, Federica Battisti, et al. Image database tid2013: Peculiarities, results and perspectives. *Signal Processing: Image Communication*, 30:57–77, 2015.
- [31] Xinwei Liu, Marius Pedersen, and Jon Yngve Hardeberg. Cid: Iq—a new image quality database. In *International Conference on Image and Signal Processing*, pages 193–202. Springer, 2014.
- [32] Wen Sun, Fei Zhou, and Qingmin Liao. Mdid: A multiply distorted image database for image quality assessment. *Pattern Recognition*, 61:153–168, 2017.
- [33] Hanhe Lin, Vlad Hosu, and Dietmar Saupe. Kadid-10k: A large-scale artificially distorted iqa database. In *2019 Eleventh International Conference on Quality of Multimedia Experience (QoMEX)*, pages 1–3. IEEE, 2019.
- [34] Domonkos Varga. Comprehensive evaluation of no-reference image quality assessment algorithms on kadid-10k database. *arXiv preprint arXiv:2010.09414*, 2020.